Hindawi
Geofluids
Volume 2019, Article ID 8639806, 10 pages
https://doi.org/10.1155/2019/8639806

Research Article

A Roadheader-Assisted Coal Cutter Based on Tensile Failure Mechanism of Coal

Bo Liu,[1,2] **Zhiliu Wang**,[1] **Wei Xu**,[1] **Zhiwei Yu**,[1] **Zhendong Yan**,[3] **and Biao Yao**[1]

[1]*School of Mechanics & Civil Engineering, China University of Mining and Technology, Beijing 100083, China*
[2]*State Key Laboratory for Geo-Mechanics and Deep Underground Engineering, Beijing 100083, China*
[3]*Jin Cheng Coal Mining Group King-ding Mining and Machinery Co. Ltd., Jincheng 048006, China*

Correspondence should be addressed to Bo Liu; 996056302@qq.com

Received 21 June 2018; Revised 15 September 2018; Accepted 30 September 2018; Published 14 January 2019

Guest Editor: Bisheng Wu

This paper proposes a new roadheader-assisted coal cutter (RACC) based on the tensile failure mechanism of coal. An innovative mining method, called the cutting inside and spalling outside mining (CISOM) method, is developed based on this new RACC. The mechanical model is established, and the working mechanism of the new CISOM method is illustrated using a column model and a beam model. The mechanical models reveal that the tensile stress causes greater deflection than compressive stress. The deflection and mining width demonstrates a quadratic relationship. To understand the stratum behaviors and improve mining efficiency, the stability of a working face owned by Jincheng Coal Mining Group in Shanxi is analyzed using UDEC numerical simulation. Numerical results indicate that the optimal values of the parameter are 0.8 m width for the inside cutting and 0.4 m width for the outside spalling at #1305 working face. The newly developed RACC was successfully applied at #1305 working face. The field results showed that the recovery rate of CISOM method is over 90%; i.e., it is improved by 20% in comparison with the traditional method.

1. Introduction

Scientized mining and green mining have attracted increasing attention as more developers have seen its benefit of high mining rate and low energy consumption [1]. For thick seam mining, this issue is even more important. However, for coal seams with complicated geological conditions, low coal recovery rate and high energy consumption have always been a problem as they affect the economic efficiency of operators.

To solve these problems, the current research aims at improving the efficiency of coal breaking, reducing mining costs and support investment, and ensuring the stability of the working face. Longwall mining has been widely adopted in both hard-rock and soft-rock mining environments [2, 3]. Longwall top coal caving (LTCC) has been well studied and widely applied in mining thick coal seams to improve recovery efficiency [4, 5], partly because caved coal was extracted from the area behind shields as well as the sheared face. Unver and Yasitli [6] suggested to uniformly fracture the top coal as much as possible to decrease the dilution and increase the extraction ratio and production efficiency. Yasitli and Unver [7] indicated that analysis of 3-D stresses around a longwall face can help increase mining efficiency. Saeedi et al. [8] suggested that increasing the size of coal pillar could secure the stability of roof and improve recovery of longwall top coal caving (LTCC). Xia et al. and Wiley [9, 10] studied the mechanisms that the borehole hydraulic coal mining system (BHCMS) causes fragmentation of coal seams using a high-pressure water jet in order to improve mining efficiency and coal recovery rate. Fourie et al. [11] discussed a new-generation XLP equipment, and higher production and greater efficiencies for mining were achieved using this equipment. The wide stall mining method [12] was proposed and demonstrated the advantages of optimizing recovery safety during thick coal exploitation by both laboratory and field investigations. Si et al. [13] introduced an intelligent multisensor data fusion identification method using the parallel quasi-Newton neural network to efficiently and accurately identify the drilling condition. The DFN

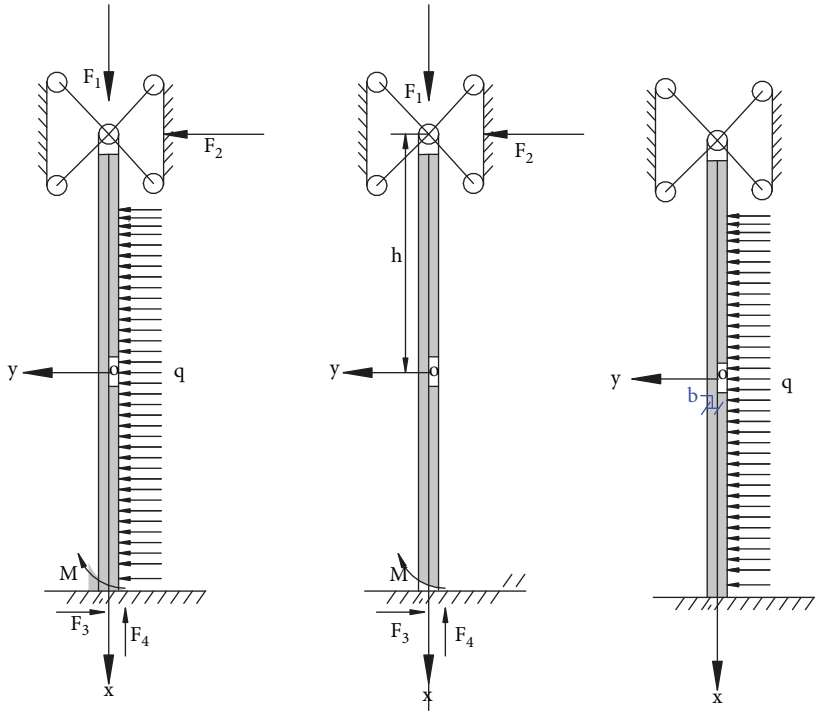

(a) Mechanical analysis of the coal wall (b) Column model (c) Beam model

Figure 1: Mechanical models.

model indicated that the P32 volumetric fracture intensity strongly controls the overall fragmentation of the rock mass, which is of great benefit to optimizing the caving process and improving the efficiency of coal mining [14]. Liu et al. [15, 16] studied the rock-breaking performance of roadheader and conical cutter and found that the rock breaking effect can be improved under the action of the water jet.

The previous studies were mainly based on the traditional compressive-shear breakage mining method. However, coals are brittle material; e.g., typically the tensile strength of a coal is only about 10% of its compressive strength. On the other hand, the research on coal's tensile fracture mechanism is limited.

To improve mining efficiency, reduce the supporting cost, and secure the stability of working face in thick coal seam conditions, in this work, we propose a new roadheader-assisted coal cutter (RACC) based on coal's tensile failure mechanism. To obtain the optimum parameters of cutting inside width and spalling outside width for #1305 fully mechanized mining face with large mining height working face of Jincheng Coal Mining Group, Shanxi, China, numerical analysis in UDEC is conducted.

2. Background

#1305 fully mechanized working face with large mining height applies the retrograde style comprehensive mechanical mining method. #3 coal is the primary minable coal seam. The design production capacity of the mine is 0.9 Mt/a. Coal seam thickness is 4.6 m~5.5 m with an average thickness of 5 m. Coal seam inclination is 1°~8°, and the average inclination is 3°. The seam is nearly flat. The mining area is 25,381 m^2. However, because of the constraints imposed by the geological structure and industrial square pillar of the power plant, the mine faced four challenges, including poor mining conditions, low mining efficiency, high energy consumption, and poor stability at the working face. Statistics show that the average mining rate per day is 2050 t/d, and the production capacity is 0.75 Mt/a, which cannot meet the design requirements. The production efficiency of the mine is too low.

Therefore, it is essential to increase the coal recovery rate by improving mining speed and reducing energy consumption during the mining process. This paper proposes a new roadheader-assisted coal cutter based on the tensile failure mechanism of coal to improve the mining efficiency. The theoretical background on the working mechanism of the new roadheader is discussed in the next section.

3. Mechanical Analysis

Coal is a brittle material, and it has relatively high compressive strength and low tensile strength. The tensile strength of coal is only about 10% of its compressive strength, and the energy required to break the coal mass by tension is much smaller than that by compression or shearing. In the process of coal failure, the coal wall may be idealized as a column model and a beam model. The coal mass is broken by the combination of roof compressive stress and the horizontal tensile stress.

The mechanical model of the coal wall is shown in Figure 1(a), which can be decomposed into two simpler submodels, i.e., a column model (Figure 1(b)) and a beam model (Figure 1(c)); the deflection of the coal wall can be obtained

using the superposition method. The column will deflect under the compressive load from the roof (F_1). The beam will also deflect under the lateral uniform load (q). The overall deflection can be achieved by superimposing the deflections obtained from these two submodels.

3.1. The Column Model. As shown in Figure 1(b), the coal sidewall is conceptualized as a column with one end fixed and the other end hinged. In the axial direction, we have $F_1 = F_4 = F$. In order to obtain the deflection of the column, the coordinate system shown in Figure 1(b) is used to describe the problem. The x-axis is in the axial compression column, and vertical downward is the positive x-direction. Taking the central point in the coal wall as the origin, we assumed that the deflection at any cross-section from the origin is ω_1. The deflection is caused by blending moment in each cross-section. If F is the absolute value, ω is positive, and M is negative, and vice versa. Therefore,

$$M(x) = \quad F\omega_1 - F_3(h + x). \tag{1}$$

The deflection curve equation of the column is

$$\frac{d^2\omega_1}{dx^2} = -\frac{M(x)}{EI}, \tag{2}$$

where E is the modulus of elasticity and I is the centroidal principal moment of the inertia of an area.

Meanwhile, substituting (1) into (2), we obtain

$$\omega_1'' = -\frac{1}{EI}[F\omega_1 - F_3(h + x)]. \tag{3}$$

Assuming that

$$k^2 = \frac{F}{EI}. \tag{4}$$

Combining the differential equations (1), (2), and (3), the deflection equation may be written as

$$\begin{aligned}
\omega_1 &= A \sin k(h - x) + B \cos k(h - x) + \frac{F_3}{F}(h + x),\\
\omega_1' &= -Ak \cos k(h - x) + Bk \sin k(h - x) + \frac{F_3}{F},\\
\omega_1'' &= -Ak^2 \sin k(h - x) + Bk^2 \cos k(h - x),
\end{aligned} \tag{5}$$

where A and B are the integral constants.

According to Sun et al. [17] and the column theory, the coal wall deflection under pure compressive load is

$$\omega_1 = \frac{2hF_3}{F_1}\left[\frac{\sin[k(h - x)]}{2h} + \cos k(h - x) + \frac{h - x}{2h}\right]. \tag{6}$$

3.2. The Beam Model. As is shown in Figure 1(c), the coal wall may be seen as a beam with one end fixed and other end hinged. The deflection is caused by the lateral uniform load q. According to Yang [18], the following stress function can be obtained:

$$\varphi = q\left[-\frac{x^2}{4} + \frac{3}{8}\frac{x^2y}{h} + \frac{y^3}{8h^3}\left(l^2 - \frac{2h^2}{5}\right)\right] - \frac{1}{8h^3}\left(x^2y^3 - \frac{y^5}{5}\right). \tag{7}$$

Taking into the boundary condition, we have

$$\begin{aligned}
&\sigma_x = \frac{q}{2J}\left[y(h^2 - x^2) + 2y\left(\frac{y^2}{3} - \frac{h^2}{5}\right)\right]\sigma_y = -\frac{q}{2J}\left(\frac{y^3}{3} - h^2y + \frac{2}{3}h^3\right),\\
&\tau_{xy} = -\frac{q}{2J}(h^2 - y^2)x.
\end{aligned} \tag{8}$$

According to the stress-strain relations, we have

$$\begin{aligned}
\frac{\partial v}{\partial x} &= \frac{hq}{EJ}\upsilon xy^2 + \frac{dv(x)}{dx},\\
\frac{\partial u}{\partial y} &= \frac{hq}{EJ}\left[(2 + \upsilon)xy^2 - \frac{x^3}{3} + \left(4h^2 - \frac{2}{5}b^2 - \upsilon b^2\right)x\right] + \frac{du(y)}{dy},\\
v(x) &= \frac{hq}{EJ}\left[\frac{1}{12}x^4 + \left(\frac{4}{5}b^2 - 2h^2 + \frac{4}{5}\upsilon b^2\right)x^2 + \left(\frac{5}{3}h^2 - \frac{2}{5}b^2 - \upsilon b^2\right)hx\right.\\
&\quad \left. + \left(\frac{h^4}{4} + \frac{8}{5}b^2h^2 + \frac{5}{2}\upsilon b^2h^2\right)h\right].
\end{aligned} \tag{9}$$

Under the interaction of the vertical compressive stress from the roof and the lateral horizontal uniform load q, the overall deflection ω of the coal wall can be calculated:

$$\begin{aligned}
\omega = v(x) + \omega_1 &= \frac{hq}{EJ}\left[\frac{1}{12}x^4 + \left(\frac{4}{5}b^2 - 2h^2 + \frac{4}{5}\upsilon b^2\right)x^2\right.\\
&\quad + \left(\frac{5}{3}h^2 - \frac{2}{5}b^2 - \upsilon b^2\right)hx + \left.\left(\frac{h^4}{4} + \frac{8}{5}b^2h^2 + \frac{5}{2}\upsilon b^2h^2\right)h\right]\\
&\quad + \frac{2hF_3}{F_1}\left[\frac{\sin k(h - x)}{4.49} + \cos k(h - x) + \frac{h - x}{2h}\right],\\
\omega'(x) &= \frac{hq}{EJ}\left[\frac{x^3}{3} + \left(\frac{8}{5}b^2 - 4h^2 + \frac{8}{5}\upsilon b^2\right)x + \left(\frac{5}{3}h^2 - \frac{2}{5}b^2 - \upsilon b^2\right)h\right]\\
&\quad + \frac{2hF_3}{F_1}\left[\frac{-k \cos k(h - x)}{4.49} - \sin k(h - x) - \frac{1}{2h}\right],
\end{aligned} \tag{10}$$

where

$$J = \frac{2}{3}\delta h^3. \tag{11}$$

In #1305 fully mechanized working face with large mining height, $h = 2.5$ m, $b = 0.6$ m, $\upsilon = 0.3$, and buried depth $H = 405$ m.

From the deflection equations above, we can see that

$$v(x) > > \omega_1(x), \tag{12}$$

which indicates that the deflection produced by the tensile stress is much greater than that produced by the compressive stress.

Assuming that ω is the maximum value and b is a parameter to be determined, then we have

$$\omega'(b) = \frac{hq}{EJ}\left[\frac{8}{5}x^2(v+1) - \left(\frac{4}{5}+2v\right)hx + \left(\frac{16}{5}+5v\right)h^3\right]b. \tag{13}$$

It can be seen that, while $b > 0$, $\omega'(b) > 0$, ω also increases with b in the form of parabolic.

The calculation results above indicate that, if the coal mining machine can break the coal by tensile stress during coal mining, its efficiency will be much higher than the traditional method which is based on the compressive failure mechanism. This method is valid for the coals which have high compressive strength and low tensile strength.

4. Roadheader Assisted Coal Cutter

Traditional drum shearer is demanding on the power because high external compressive and shear stresses are required to be applied on the coal mass for direct cutting. Additionally, compressive and shear stresses may cause severe stratum behavior and threaten stability of working face. The theoretical analysis in the section above indicated that for the same power consumption, the tensile stress induces larger deflection than compressive stress. To improve the mining efficiency, we propose a new mining method called cutting the inside and spalling outside mining (CISOM) method based on the principle of tensile fracture mechanism.

This tensile failure-based RACC is innovative as no similar approaches have been proposed before; i.e., it overturns the traditional concept of coal mining in which coal mass is broken by compressive shearing failure. Application of this RACC in #1305 working face made its production capacity increase to 2500 t/d from 2050 t/d (with traditional shearer) and coal mining rate increase by 20%. The power of new roadheader-assisted coal cutter is only 0.67 times that of the traditional shearer. The main technical parameters of the new RACC are shown in Table 1.

Note that this new RACC can be applied in both thin and thick coal seams.

The components and filed schematic diagrams of the new roadheader-assisted coal cutter are shown in Figures 2 and 3. The key components are 1 and 7. The cutting head has blades for cutting coal directly by applying compressive and shear stress on the coal. The cutting arm spalls the coal behind the cutting head. The web depth is usually 1200 mm for both the traditional and the new roadheader-assisted coal cutters. The traditional shearer achieves mining coal by drum rotation. The new roadheader-assisted coal cutter, however, first cuts 800 mm web depth of the coal using the cutting head (part I, Figure 4), then spalls 400 mm web depth of the coal (part II, Figure 4). The mining of part I is called cutting inside; it is based on the compressive-shear failure which is similar to the principle of the traditional mining methods. The mining of part II is called spalling outside. It is relatively easy to crush the coal using this part because of the combined effect of roof pressure, the coal's self-gravity, and the tensile stress by the cutting arm. Based on its working process, this method is called the DSIOM method. Figure 5 shows the layout of the CISOM method. Figure 4 shows the A-A profile, and Figure 6 shows the top view.

Table 1: Main technical parameters of the new RACC.

Main technical index	Parameters
Production capacity (t/h)	250
Mining height (m)	2.4~5.6
Drum diameter (mm)	$\Phi = 800$
Web depth (m)	1.2
Total installed power (kW)	190
Size (mm)	4700*2370*2342 (length*width*height)

5. Numerical Simulations

In order to further study the impact of parameters on the stability, the numerical simulation is carried out in UDEC to analyze the stability at #1305 working face of Jincheng Coal Mining Group in Shanxi, China. A numerical model mesh of rock mass after excavation is shown Figure 7. The model extensions are 50 m × 36 m. When the part of "cutting inside" in Figure 7 is mined, the obvious bending shows that the "spalling outside" is easy to crush. Roller boundary condition is applied to the lateral and bottom boundaries of the model. A vertical stress of 10.3 MPa is applied on the top boundary of the model to simulate the overburden load. Meanwhile, the Mohr-Coulomb constitutive model is assigned to the numerical model. The material parameters in the numerical simulation are summarized in Table 2.

In order to analyze the stability, the deflections of the roof squad and the coal wall are monitored at different monitoring points. The horizontal monitoring points are installed in the upper part of the coal wall to monitor the roof squat, and the distances away from the working face are 0 m to7m with an interval of 0.5 m. The vertical monitoring points are installed in the coal wall to monitor deflection, and the distances away from the roof are 0 m to 5 m with a spacing of 0.5 m. Figure 8 shows the horizontal points from R1 to R15 and vertical monitoring points from W1 to W11.

The schemes of different cutting widths are simulated from 0.4 m to1.2 m. The relatively optimal parameters of CISOM are obtained by comparing the deflections of the roof squad and coal wall under different schemes as shown in Table 3. The width of plastic zone, the roof squat, and the maximum deflection of the coal wall are analyzed. The results are shown in Figures 9–11, respectively.

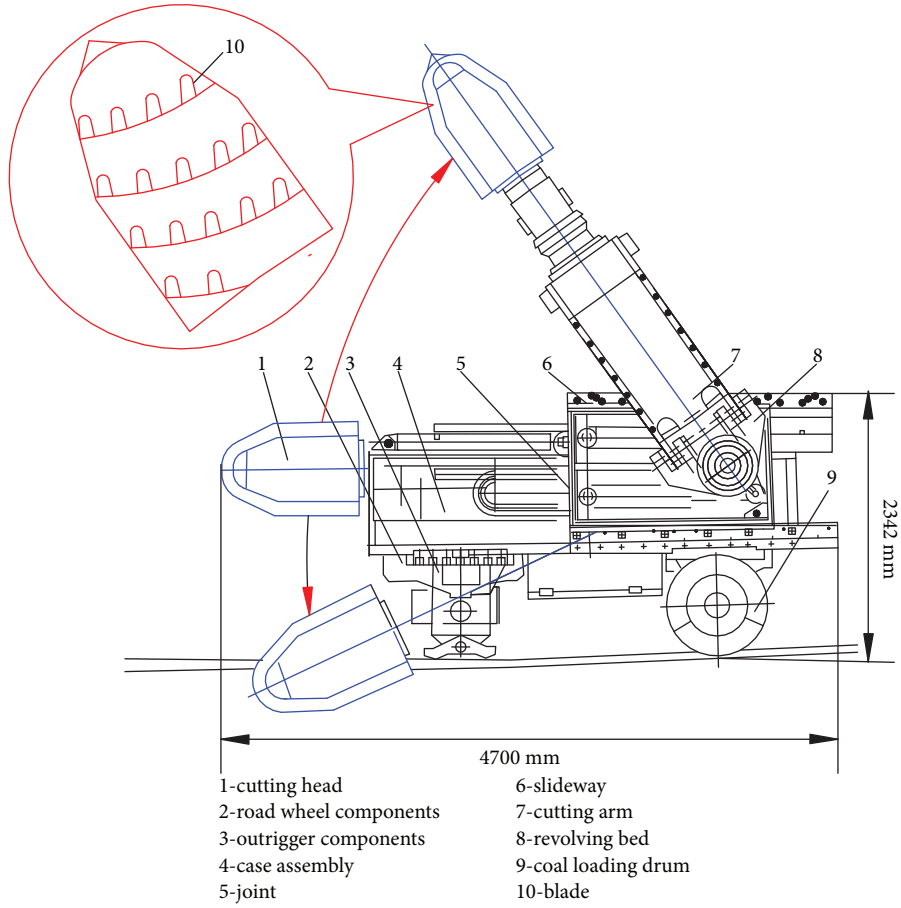

Figure 2: Components of the new roadheader-assisted coal cutter.

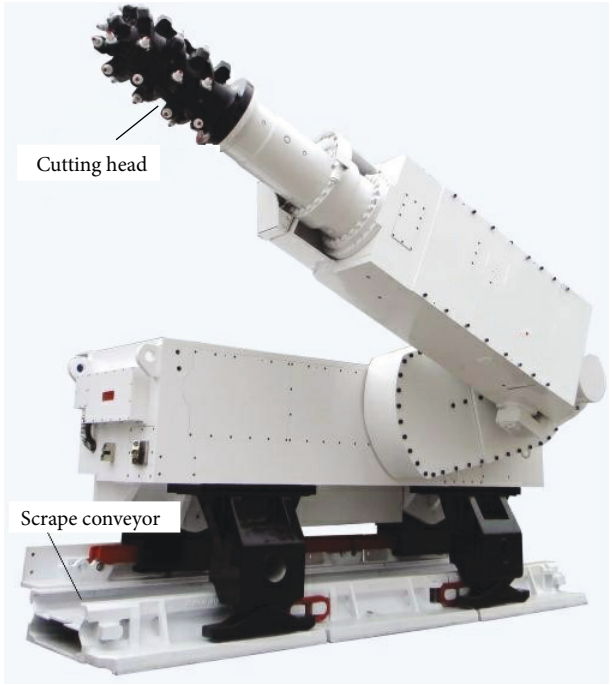

Figure 3: Field schematic diagrams of the new roadheader-assisted coal cutter.

As seen in Figures 9–11, as the tensile strength decreases, the plastic area in coal mass increases, which indicates that the smaller width makes this part of the coal easier to be spalled. When the cutting width is about 0.8 m, the plastic area increases significantly. However, the expanded plastic area will threaten the stability of the working face. The max deflection of the coal wall is 98.14 mm, 100.35 mm, 103.41 mm, 121.5 mm, 141.5 mm, 185.8 mm, 203.1 mm, and 221.2 mm from scheme 1 to scheme 8, respectively. With the increase of the cutting width and the decrease of the spalling width, the max deflection of the coal wall increases gradually. When the cutting width is more than 0.8 m, #1305 working face has the risk of running into instability. The max deflection of the coal wall shows an approximate parabolic increasing trend, which matches the theoretical analysis above. The deflection of the coal wall shows the similar trend.

In summary, for #1305 fully mechanized work face with large mining height, in order to ensure the stability of the working face, the optimum parameter value for CISOM method is to set the cutting inside width to 0.8 m and spalling outside width to 0.4 m.

6. Practical Application

To explore the practical application of cutting inside width as 0.8 m and spalling outside width as 0.4 m at #1305 working

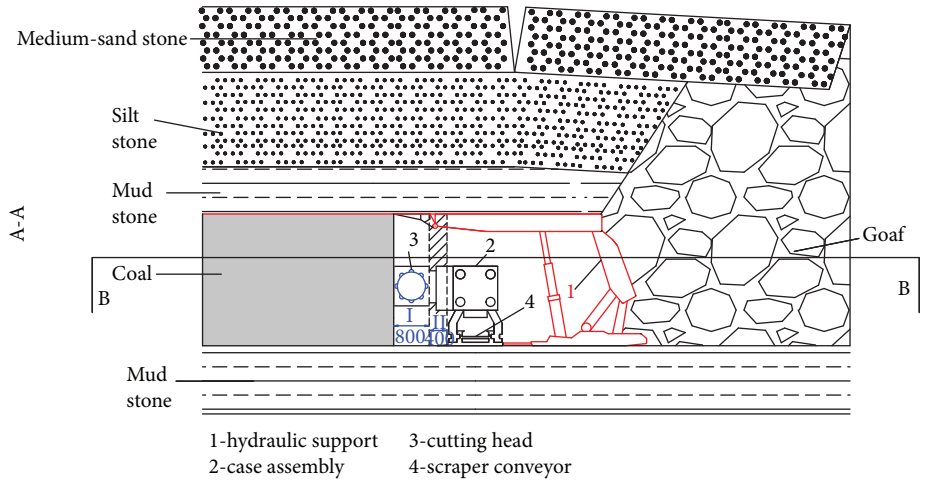

Figure 4: Working mechanism (A-A profile).

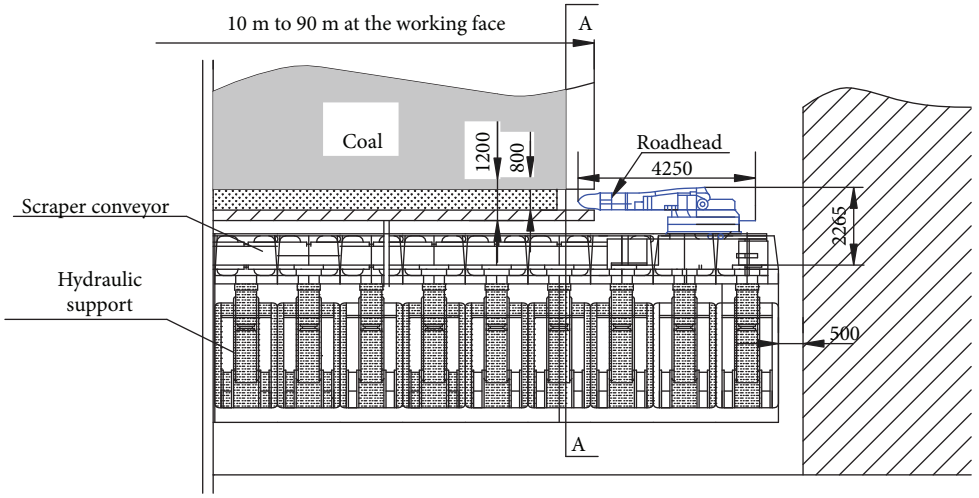

Figure 5: The field layout of the CISOM method.

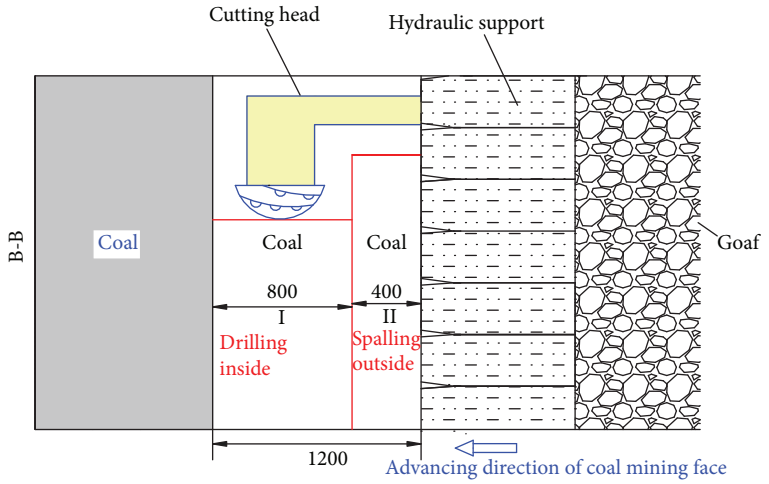

Figure 6: Working mechanism (top view).

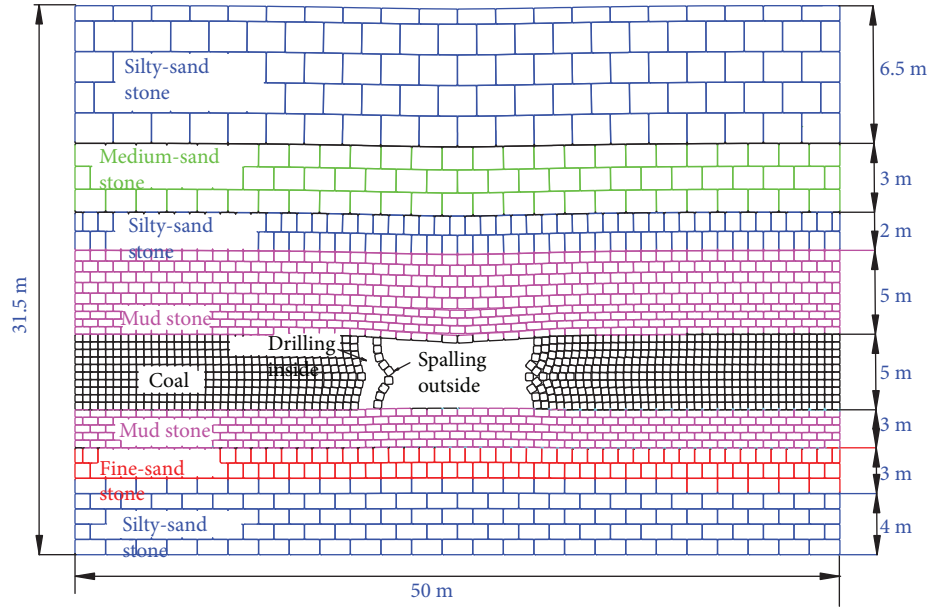

Figure 7: Rock grids after excavation.

Table 2: Physical mechanic parameters.

Lithology	Bulk (GPa)	Shear (GPa)	Friction (°)	Cohesion (MPa)	Tensile (MPa)	Density (kg/m^3)
Fine-sand stone	11.2	5.9	27.56	2.21	9.19	2510
Silty-sand stone	14.4	7.5	33	2.42	9.43	2431
Medium-sand stone	15.5	7.9	26	2.32	9.21	2287
Mud stone	8.2	4.3	23	4.3	8.65	2400
3# coal	5.1	2.6	24.8	1.3	3.1	1450

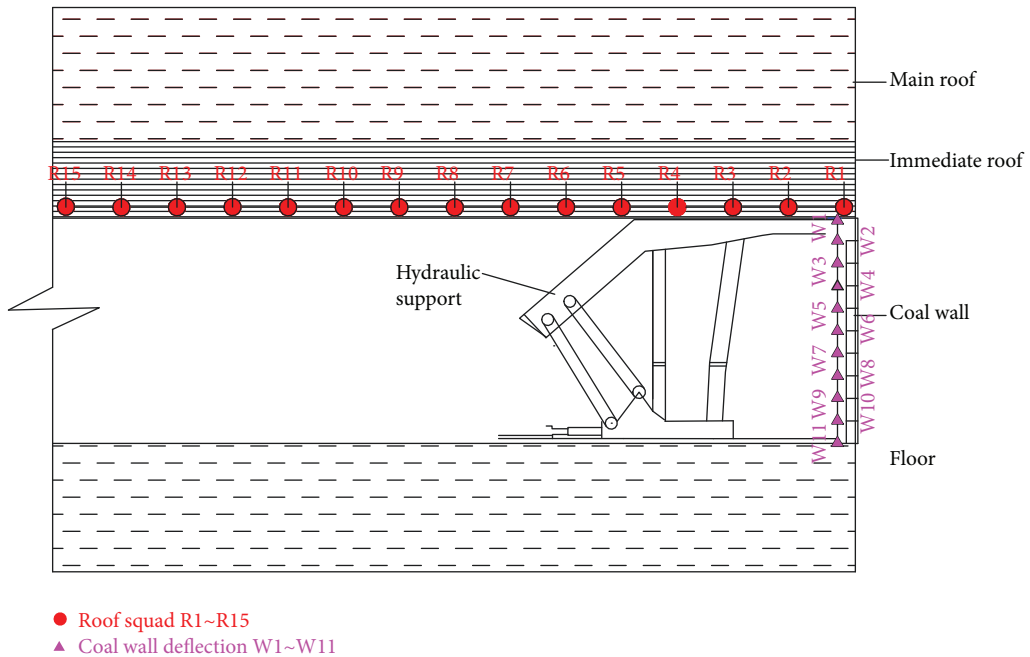

Figure 8: Monitoring points.

Table 3: Simulation scheme.

Scheme	Spalling width (m)	Cutting width (m)	Scheme	Spalling width (m)	Cutting width (m)
1	0.4	0.8	**5**	0.8	0.4
2	0.5	0.7	**6**	0.9	0.3
3	0.6	0.6	**7**	1	0.2
4	0.7	0.5	**8**	1.2	0

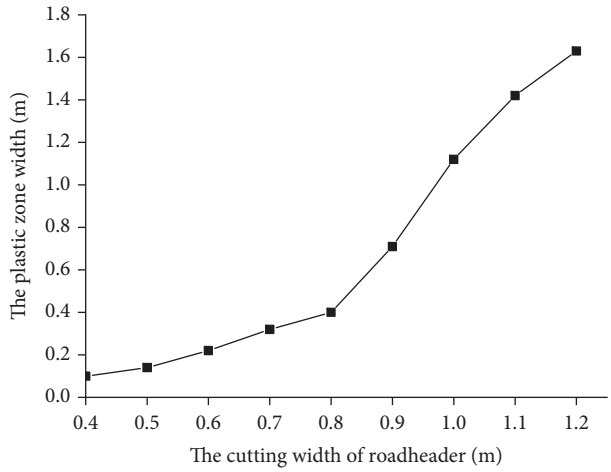

Figure 9: Plastic zone width versus cutting width.

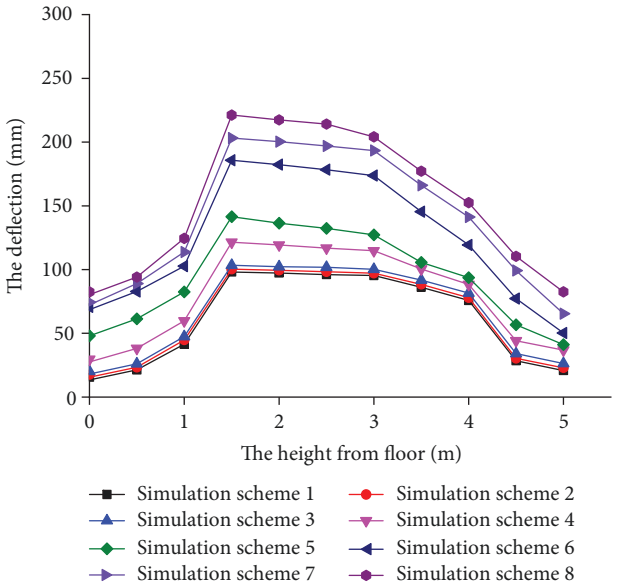

Figure 10: The deflection versus cutting width.

face, the resistance distribution of hydraulic supports and economic benefits are studied. The percentage of statistical work resistance in each section is analyzed according to mass data recorded by computers which are about 80,000 data sets recorded in each group.

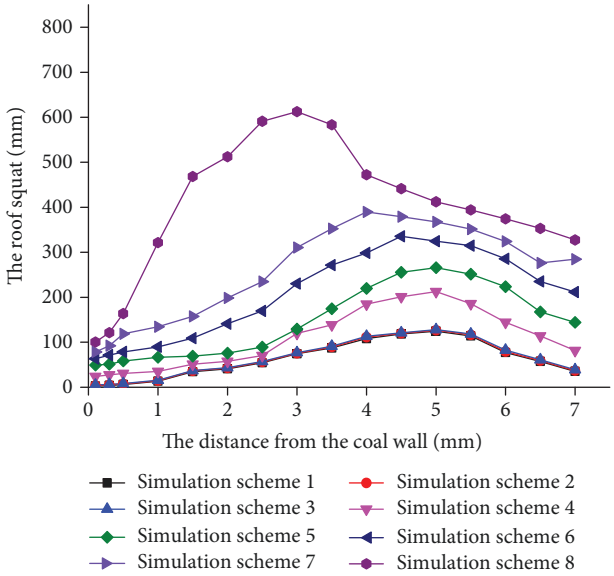

Figure 11: Roof squad versus cutting width.

The circulation end resistance is the last working resistance of the hydraulic supporter when the working face advances forward in one round of excavation. The circulation end resistance distribution of hydraulic supports is shown in Figure 12. The distribution of the circulation end resistance is dispersed, and its average is about 2000 kN. Moreover, more than half of hydraulic supports are above 2500 kN. The maximum circulation end resistance is more than 5000 kN. Only a few hydraulic supports have load significantly larger than the rated working resistance of 5500 kN. The above analysis shows the hydraulic support can meet the requirements of roof support and the working face is in a stable state.

The weighted working resistance distribution of hydraulic supports is shown in Figure 13. The average distribution of time-weighted working resistance is relatively centralized between 2000 and 3000 kN. There are a few hydraulic supports whose maximum working resistance is obviously higher than rated working resistance (5500 kN). Therefore, the hydraulic support meets the requirements of roof support.

According to the field test, the following conclusions may be drawn:

(1) The new RACC can greatly improve the coal mining efficiency at the working face thus resulting in significant economic benefits. If the designed mine capacity is 0.9 Mt/a, in comparison with the traditional shearer which is based on compressive-shear failure (recovery rate is 60%~70%), the recovery rate of the new RACC is over 90% and the mining height is 6 m. According to coal mining capacity per day, the recovery rate in the working face is improved by 20%. The increased profit is 73 million yuan (RMB) per year when the new CISOM method is applied for #1305 fully

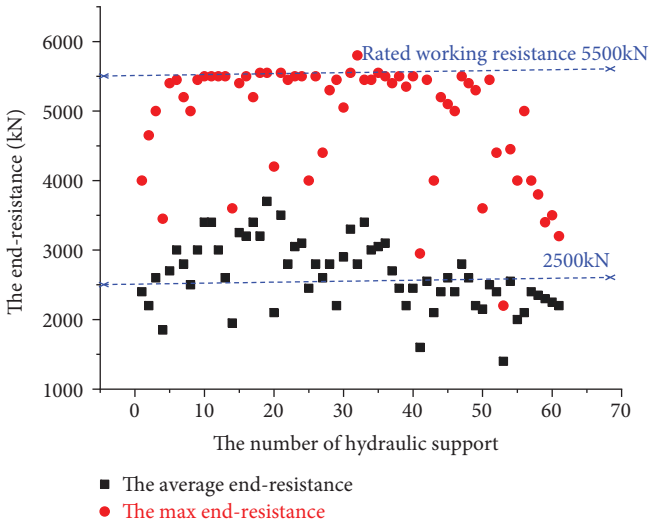

Figure 12: The circulation end resistance distribution of hydraulic supports.

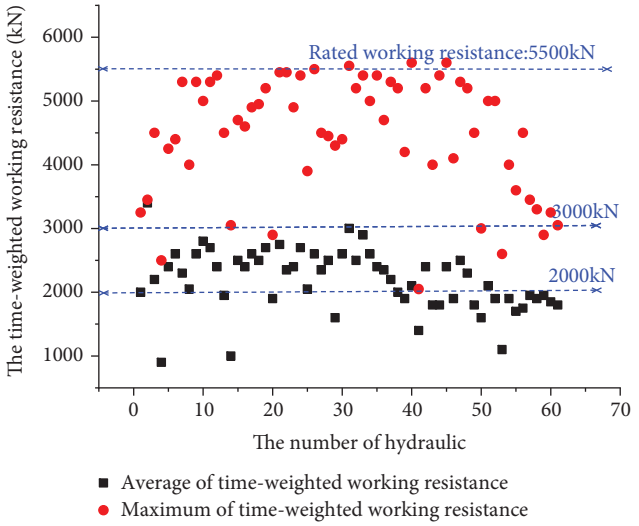

Figure 13: The weighted working resistance distribution of hydraulic supports.

mechanized working face of Jincheng Coal Mining Group, Shanxi, China

(2) Based on the field test, the work resistance and end resistance of hydraulic support are within the allowable range. The new CISOM method based on tensile failure mechanism can improve the safety of working face and reduce underground pressure. Meanwhile, the new CISOM method can better secure the stability of the roof and coal wall and ensure the rapid advancement at the working face

In summary, the field test of #1305 working face shows that the CISOM method by using RACC not only is more efficient but also can ensure the stability of the working face.

7. Conclusions

In this work, the mechanical principles of the tensile failure mechanism based RACC are explained and then a practical application is presented. The following conclusions may be drawn:

(1) The beam model indicates that the deflection of coal mass at the working face caused by tensile stress is larger than that caused by compressive stress. Meanwhile, the deflection ω and the width obey a parabolic relationship. The theory shows that the CISOM method by using RACC is relatively easier for mining coal than the traditional shearer mining method.

(2) An innovative roadheader-assisted coal cutter by applying tensile stress on the coal is proposed for the first time. It is totally different from the traditional concept of mining coal and induces coal fracture by compressive stress. Based on a practical application case study, the production capacity of a working face is increased by 20%. Additionally, the new roadheader-assisted coal cutter can be applied on both thin and thick coal seams.

(3) The numerical analysis of the stability of a work face demonstrates that the optimum parameter value for this CISOM method is to choose the cutting inside width as 0.8 m and spalling outside width as 0.4 m.

(4) The field observations show that the new roadheader-assisted coal cutter has the advantages of improving mining efficiency. The recovery rate is improved by 20% for #1305 fully mechanized working face owned by Jincheng Coal Mining Group, Shanxi, China.

Symbols

Φ: Stress function (N)
q: Lateral uniform load (N/m^2)
F_1: Roof compressive force (N)
F_2: Horizontal force in the coal roof (N)
F_4: Vertical supporting force in the coal seam floor (N)
M: Bending moment (N·m)
h: Half of mining height (m)
I: Centroidal principal moment of inertia of an area (m^4)
b: Half of mining width (m)
ω: Overall deflections of coal wall (m)
u: Deflection in the x direction (m)
v: Deflection in the y direction (m)
F_3: Horizontal force in the coal floor (N)
E: Modulus of elasticity (Pa)
σ_x: Stress in the x direction (Pa)
τ_{xy}: Shear stress (Pa)
ω_1: Coal wall deflection for the pure compression bar (m)
δ: Thickness of the coal wall (m).

Data Availability

The data used to support the findings of this study are available from the corresponding author upon request.

Conflicts of Interest

The authors declare that there is no conflict of interest regarding the publication of this paper.

Acknowledgments

The authors sincerely thank the following agents for their financial supports: National Natural Science Foundation of China (41472259 and 51274209) and the 13th Five-Year Period National Key Research and Development Program of China (2016YFC080250504).

References

[1] H. Q. Shi, "Mine green mining," *Energy Procedia*, vol. 16, Part A, pp. 409–416, 2012.

[2] H. Wang, Y. Jiang, Y. Zhao, J. Zhu, and S. Liu, "Numerical investigation of the dynamic mechanical state of a coal pillar during longwall mining panel extraction," *Rock Mechanics and Rock Engineering*, vol. 46, no. 5, pp. 1211–1221, 2013.

[3] A. Vakili and B. K. Hebblewhite, "A new cavability assessment criterion for longwall top coal caving," *International Journal of Rock Mechanics and Mining Sciences*, vol. 47, no. 8, pp. 1317–1329, 2010.

[4] H. Alehossein and B. A. Poulsen, "Stress analysis of longwall top coal caving," *International Journal of Rock Mechanics and Mining Sciences*, vol. 47, no. 1, pp. 30–41, 2010.

[5] M. Khanal, D. Adhikary, and R. Balusu, "Prefeasibility study-geotechnical studies for introducing longwall top coal caving in Indian mines," *Journal of Mining Science*, vol. 50, no. 4, pp. 719–732, 2014.

[6] B. Unver and N. E. Yasitli, "Modelling of strata movement with a special reference to caving mechanism in thick seam coal mining," *International Journal of Coal Geology*, vol. 66, no. 4, pp. 227–252, 2006.

[7] N. E. Yasitli and B. Unver, "3-D numerical modelling of stresses around a longwall panel with top coal caving," *Journal of the Southern African Institute of Mining and Metallurgy*, vol. 105, no. 5, pp. 287–300, 2005.

[8] G. Saeedi, K. Shahriar, B. Rezai, and C. Karpuz, "Numerical modelling of out-of-seam dilution in longwall retreat mining," *International Journal of Rock Mechanics and Mining Sciences*, vol. 47, no. 4, pp. 533–543, 2010.

[9] B. Xia, X. Zeng, and Z. Mao, "Research on one borehole hydraulic coal mining system," *Earth Science Frontiers*, vol. 15, no. 4, pp. 222–226, 2008.

[10] M. A. Wiley, "Borehole mining: getting more versatile," *Mining Engineering*, vol. 303, no. 1, pp. 33–36, 2004.

[11] F. Fourie, P. Valicek, G. Krafft, and J. Sevenoaks, "Narrow-reef mechanized mining layout at Anglo American platinum," *Journal of the Southern African Institute of Mining and Metallurgy*, vol. 117, no. 3, pp. 263–274, 2017.

[12] R. Singh and T. N. Singh, "Wide stall mining for optimal recovery of coal from a thick seam under surface features," *International Journal of Rock Mechanics and Mining Sciences*, vol. 36, no. 2, pp. 155–168, 1999.

[13] L. Si, Z. Wang, X. Liu, C. Tan, J. Xu, and K. Zheng, "Multi-sensor data fusion identification for shearer cutting conditions based on parallel quasi-Newton neural networks and the Dempster-Shafer theory," *Sensors*, vol. 15, no. 11, pp. 28772–28795, 2015.

[14] S. Rogers, D. Elmo, G. Webb, and A. Catalan, "Volumetric fracture intensity measurement for improved rock mass characterisation and fragmentation assessment in block caving operations," *Rock Mechanics and Rock Engineering*, vol. 48, no. 2, pp. 633–649, 2015.

[15] S. Liu, Z. Liu, X. Cui, and H. Jiang, "Rock breaking of conical cutter with assistance of front and rear water jet," *Tunnelling and Underground Space Technology*, vol. 42, pp. 78–86, 2014.

[16] Z. H. Liu, C. L. du, Y. L. Zheng, Q. B. Zhang, and J. Zhao, "Effects of nozzle position and waterjet pressure on rock-breaking performance of roadheader," *Tunnelling and Underground Space Technology*, vol. 69, pp. 18–27, 2017.

[17] X. F. Sun, X. S. Fang, and L. T. Guan, "Material mechanics," Higher education press, 4th edition, 2009.

[18] G. T. Yang, *Elastic-Plastic Mechanics Introduction*, Tsinghua University press, 2th edition, 2013.